Tectonics®

RESEARCH ARTICLE
10.1029/2022TC007531

Key Points:

- Rb-Sr multimineral ages indicate that the uppermost tectonic unit of the Saih Hatat window underwent high-pressure (HP) metamorphism before 99-96 Ma
- The cold ≥99-96 Ma HP rocks formed at the same time as the melting of the metamorphic sole in the Samail subduction zone
- Thermal consideration demand that the HP rocks and the metamorphic sole formed in two different subduction zones

Supporting Information:

Supporting Information may be found in the online version of this article.

Correspondence to:

U. Ring,
uwe.ring@geo.su.se

Citation:

Ring, U., Glodny, J., Scharf, A., & Hansman, R. (2023). Some like it cold: The "conundrum of Samail" revisited. *Tectonics*, *42*, e2022TC007531. https://doi.org/10.1029/2022TC007531

Received 10 AUG 2022
Accepted 31 DEC 2022

Author Contributions:

Conceptualization: Uwe Ring
Formal analysis: Johannes Glodny, Reuben Hansman
Funding acquisition: Uwe Ring
Investigation: Uwe Ring, Andreas Scharf
Methodology: Johannes Glodny
Project Administration: Uwe Ring
Writing – original draft: Uwe Ring
Writing – review & editing: Johannes Glodny, Andreas Scharf, Reuben Hansman

Some Like It Cold: The "Conundrum of Samail" Revisited

Uwe Ring[1], Johannes Glodny[2], Andreas Scharf[3], and Reuben Hansman[1]

[1]Department of Geological Sciences, Stockholm University, Stockholm, Sweden, [2]GFZ German Research Centre for Geosciences, Potsdam, Germany, [3]Department of Earth Sciences, Sultan Qaboos University, Al-Khod, Oman

Abstract Most tectonic models consider that the "Samail subduction zone" was the only subduction zone at the mid-Cretaceous convergent Arabian margin. We report four new Rb-Sr multimineral isochron ages from high-pressure (HP) rocks and a major shear zone of the uppermost Ruwi-Yiti Unit of the Saih Hatat window in the Oman Mountains of NE Arabia. These ages demand a reassessment of the intraoceanic suprasubduction-zone evolution that formed the Samail Ophiolite and its metamorphic sole in the Samail subduction zone. Our new ages constrain waning HP metamorphism of the Ruwi subunit at ~99-96 Ma and associated deformation in the Yenkit shear zone between ~104 and 93 Ma. Our ages for late stages of deformation and HP metamorphism (thermal gradients of ~8–10°C km^{-1}) overlap with published ages of ~105-102 Ma for Samail-subduction-zone prograde-to-peak metamorphism (thermal gradients of ~20–25°C km^{-1}), subsequent decompressional partial melting of the metamorphic sole and suprasubduction-zone crystallization of the Samail Ophiolite (thermal gradients of ~30°C km^{-1}) between ~100 and 93 Ma. Thermal considerations demand that two subduction zones existed at the mid-Cretaceous Arabian margin. High-pressure metamorphism of the Ruwi-Yiti rocks occurred in a mature, thermally equilibrated "Ruwi subduction zone" that formed at ~110 Ma. Initiation of the infant, thermally unequilibrated and, thus, immature, outboard intraoceanic Samail subduction zone occurred at ~105 Ma. The Samail Ophiolite and its metamorphic sole were then thrust over the exhuming Ruwi-Yiti HP rocks and onto the Arabian margin after ~92 Ma, while the bulk of the Saih Hatat HP rocks below the Ruwi-Yiti Unit started to be underthrust in the Ruwi subduction zone.

Plain Language Summary The Oman Mountains are famous because the oceanic lithosphere, with the boundary between the outer crust and the subcrustal mantle, is exposed at the Earth surface. This oceanic lithosphere formed above the Samail subduction zone, which is generally considered as the only subduction zone at the NE margin of Arabia in Oman during the late Cretaceous. We show, using Rb-Sr geochronology, that there must have been two subduction zones.

1. Introduction

The "conundrum of Samail" (Hacker & Gnos, 1997) refers to the interaction of "hot" processes of subduction initiation with "cold" high-pressure (HP) metamorphism in the Oman Mountains. Hacker and Gnos (1997) discussed the example of the far-traveled, non-HP Samail Ophiolite and its underlying high-temperature (HT) metamorphic sole that formed above an infant, hot, intraoceanic subduction zone and overlies the cold, continental Saih Hatat HP complex that originated in a mature subduction setting (Figures 1 and 2).

The onset of intraoceanic subduction is associated with the formation of a metamorphic sole (i.e., HT rocks subsequently welded to the base of the suprasubduction-zone ophiolite) reflecting elevated, transient thermal gradients (e.g., Dewey & Bird, 1971; Stern & Bloomer, 1992), which in the intraoceanic Samail subduction zone at the northeastern Arabian margin in Oman were up to ~30°C km^{-1} (e.g., Garber et al., 2020; Searle & Cox, 2002). The available age data constraining high-grade metamorphism and partial melting of the metamorphic sole and subsequent formation of the Samail Ophiolite (Garber et al., 2020; Guilmette et al., 2018; Rioux et al., 2021; Soret et al., 2022) demonstrate hot subduction-zone processes between 105 and 93 Ma (Figure 3). Compiled data from 70 subduction zones by Lallemand and Arcay (2021) and numerical modeling by Peacock (1990) indicate that it takes 5–15 Ma between hot subduction-zone initiation and self-sustained, steady-state subduction characterized by a stable, low-thermal gradient of ~10°C km^{-1}.

The almost completely exposed Saih Hatat window (Figure 2) represents a formidable example of a HP complex and provides a one-of-a-kind natural laboratory important for understanding subduction-zone processes. A shortcoming of the Saih Hatat HP rocks is its controversial and incomplete geochronology. Almost all geochronologic

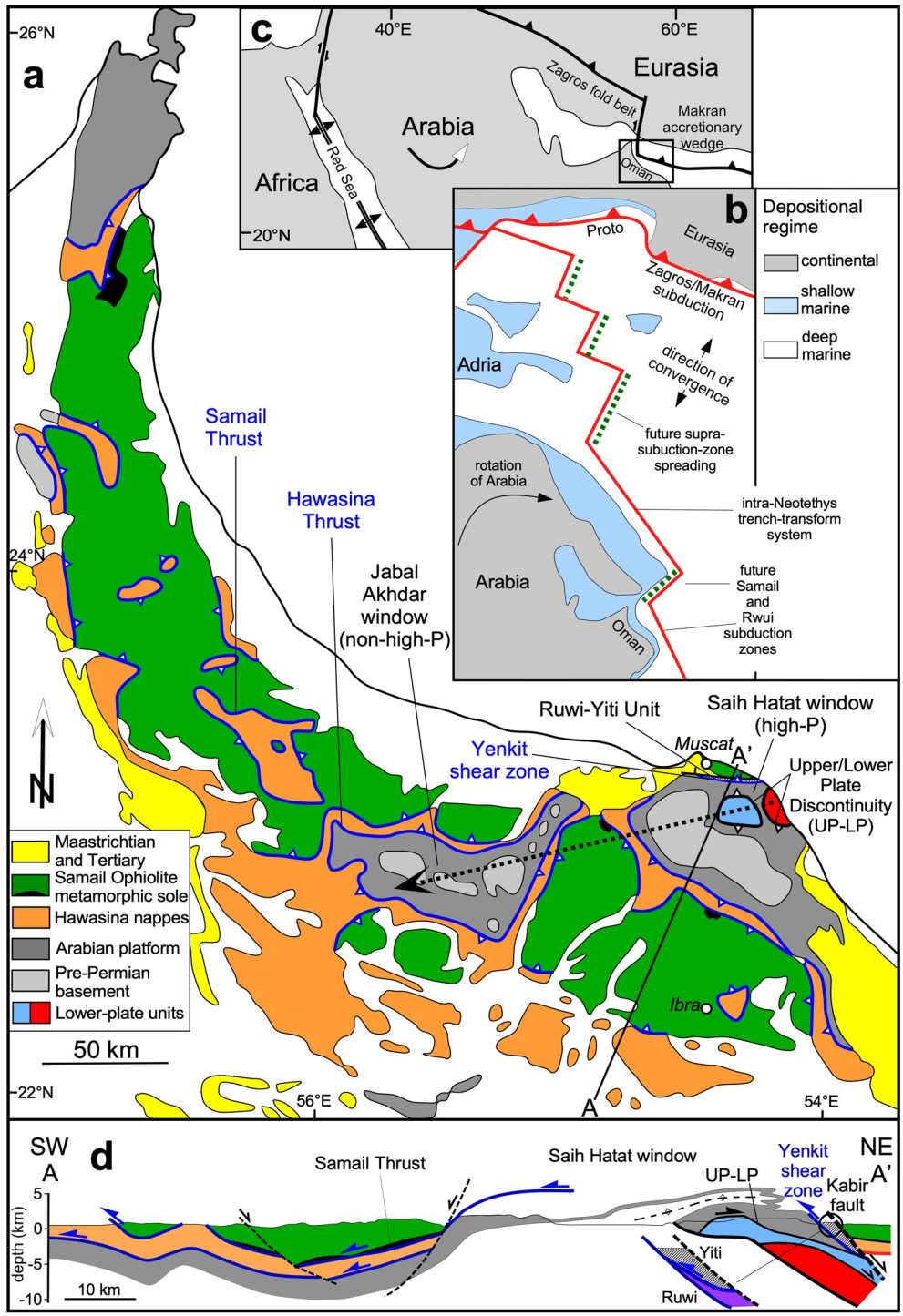

Figure 1. (a) Geology of Oman Mountains at NE margin of Arabia; Saih Hatat high-pressure (HP) window at base overlain by non-HP Samail Ophiolite and Hawasina nappes; metamorphic grade in windows decreases toward SW (dashed arrow), lower plate units of Saih Hatat window are below Upper/Lower Plate Discontinuity (blueschist-facies (blue) and eclogite-facies (red) rocks); note small, scattered outcrops of metamorphic sole (black) at base of ophiolite. Hawasina thrust separates HP from non-HP rocks; thrusts in blue refer to ~110–90 Ma, thrust and normal faults in black to post-~90 Ma tectonic history. (b) Early Cretaceous plate tectonic configuration, paleogeography and "proto" Zagros/Makran subduction system of Arabian part of Neotethys (from van Hinsbergen et al. (2021)); position of future Samail subduction zone along transform zone (Hacker et al., 1996; van Hinsbergen et al., 2019); intra-Neotethys trench-transform system according to van Hinsbergen et al. (2021). Note NNE convergence direction in Neotethys. (c) Current plate-tectonic setting of Arabian Plate and position of map in (a). (d) Simplified NE-SW cross section showing HP units below non-HP Samail Ophiolite and Hawasina nappes (modified from Searle et al. (2022)).

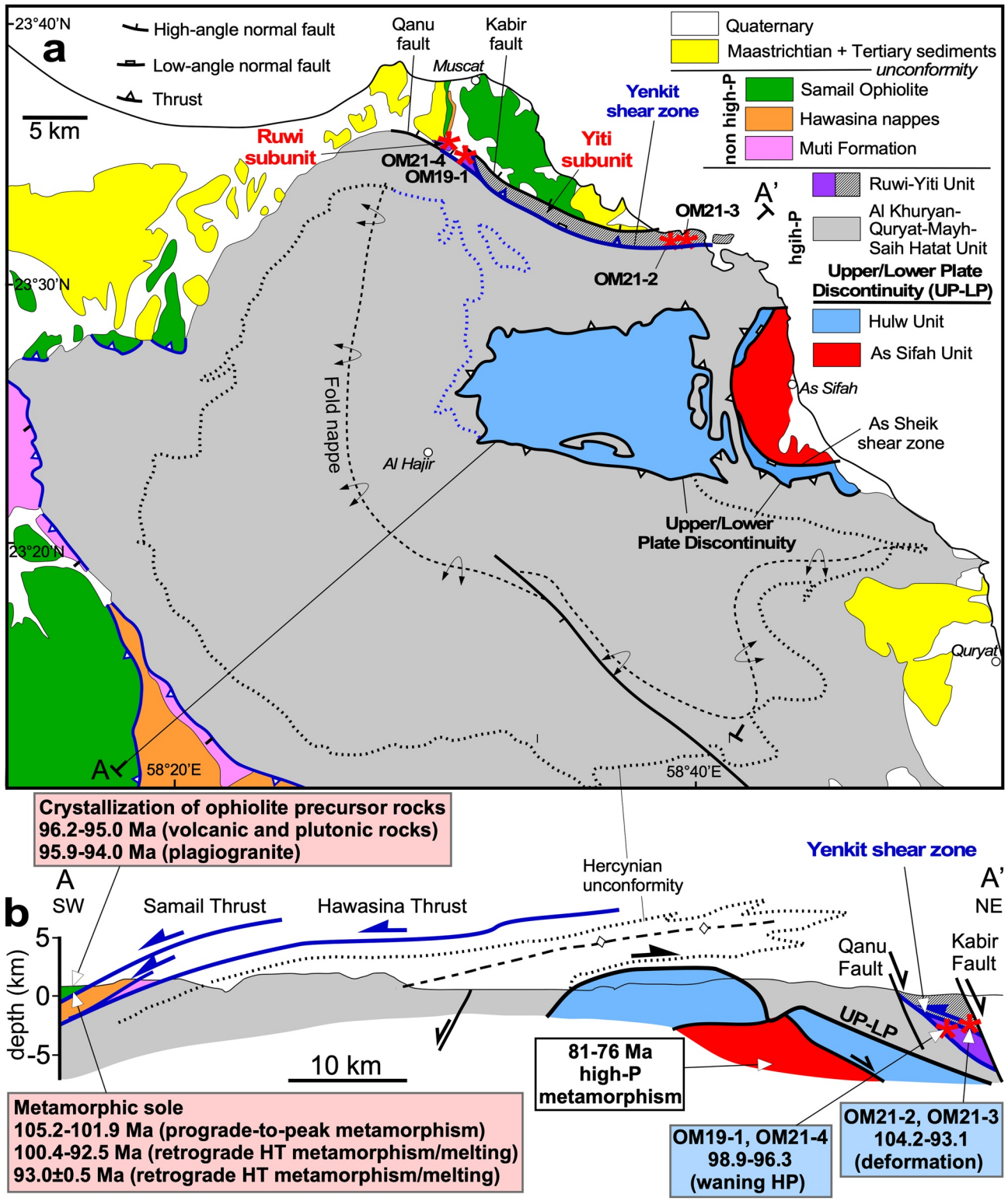

Figure 2.

studies have focused on the structurally lowest (As Sifah) tectonic unit of the nappe stack (reviews in Goscombe et al. (2020) and Hansman et al. (2021)). Prograde to peak HP metamorphism of the As Sifah Unit occurred between 81 and 76 Ma (El-Shazly et al., 2001; Garber et al., 2021; Warren et al., 2003, 2005). Most workers

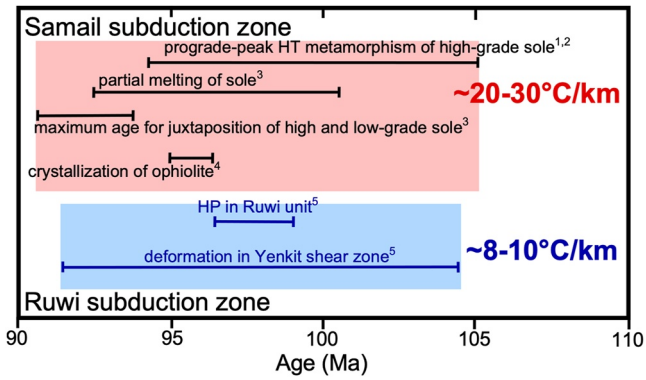

Figure 3. Ages for prograde high-temperature (HT) metamorphism and partial melting of metamorphic sole and ophiolite crystallization; juxtaposition of high- with low-grade sole proxy for end of HT conditions in Samail subduction zone. Range of ages for "cold" high-pressure metamorphism and deformation in Ruwi-Yiti Unit overlapping with "hot" conditions in Samail subduction zone. [1]Guilmette et al. (2018), [2]Soret et al. (2022), [3]Garber et al. (2020), [4]Rioux et al. (2021), [5]this study.

make the simplifying assumption that ages of 81-76 Ma date HP metamorphism across the entire Saih Hatat window (e.g., Agard et al., 2010; Garber et al., 2020; Hansman et al., 2021). However, in nearly all mountain belts worldwide, HP metamorphism is not synchronous across the entire orogen; there is typically an age progression from top to bottom of the orogen (e.g., Glodny & Ring, 2022; Liu et al., 2009; Ring & Layer, 2003; Vitale Brovarone & Herwartz, 2013). If so, units structurally above the As Sifah Unit (Figure 2) may have an older HP overprint, which would have immediate relevance for the "conundrum of Samail."

2. Setting

The closure of "Arabian" Neo-Tethys since the early Cretaceous has mostly been accommodated by northward subduction along a Eurasian "proto Zagros/Makran" subduction system (review in Burg (2018)) (Figure 1b). At the southern end of Neo-Tethys, mid/late Cretaceous convergence was accomplished in its early stages by inferred short-lived (~25 Ma) subduction/obduction processes near the northern margin of Arabia in Oman (Hacker, 1991; Hacker et al., 1996; Searle et al., 1994; van Hinsbergen et al., 2015). This Samail subduction zone rotated >90° clockwise due to subduction rollback before the Samail Ophiolite was obducted onto the Arabian Platform (Morris et al., 2016; van Hinsbergen et al., 2019, 2021).

The convergent margin in Oman is tectonometamorphically made up by two main divisions: (a) the Samail Ophiolite (with its metamorphic sole) and the underlying Hawasina nappes, which constitute the non-HP overriding plate structurally above, (b) the HP nappes of the Saih Hatat window (Figure 1).

2.1. Non-High-Pressure Overriding Plate

The overriding plate comprises the Permo-Mesozoic Hawasina nappes, with intercalated "Oman Exotics" and the Samail Ophiolite (e.g., Glennie et al., 1974). The thickness of the Semail Ophiolite varies between ~10 and 5 km (Béchennec et al., 1992; Scharf et al., 2021; Weidle et al., 2022). The original thickness of the ophiolite is unknown. Aldega et al. (2017, 2021) showed that the overburden of the entire allochthonous units in the Jabal Akhdar dome did not exceed 10–12 km.

At the interface between the ophiolite and the most distal Hawasina rocks is a metamorphic sole under the Samail Ophiolite (e.g., Ambrose et al., 2021; Cowan et al., 2014; Garber et al., 2020; Guilmette et al., 2018), which displays an inverse metamorphic gradient with granulite-facies at its top and greenschist-facies rocks at its base. The strongly sheared and attenuated remnants of the metamorphic sole delineate the thrust zone that emplaced the Samail Ophiolite (Searle et al., 2022).

2.1.1. Pre-Subduction Architecture of the Arabian Margin and the Hawasina Basin

The pre-subduction architecture of the Arabian rifted margin guided the structure of the non-HP overriding plate (Figure 4) (Béchennec et al., 1990; Blechschmidt et al., 2004; Searle, 2007). Two rifting phases in the late Permian and mid/late Triassic deformed and structured the margin. The late Permian rifting phase affected the Arabian platform and inner margin forming the intracontinental Hamrat Duru Basin bordered oceanward by the Kawr-Misfah Platform (Misfah for short). A second, mid/late Triassic rifting event affected the outer Hamrat Duru Basin, forming the Al Aridh Trough, which separated the Hamrat Duru Basin from the Misfah Platform (Béchennec et al., 1990). The latter is a rifted segment of the Arabian Platform. This rifting episode also created

Figure 2. (a) Saih Hatat window made up, from bottom to top, by As Sifah, Hulw, Mayh-Khuryan-Quryat-Saih Hatat and Ruwi-Yiti units (adapted from Le Métour, De Gramont, and Villey (1986); Le Métour, De Gramont, Villey, and Beurrier (1986); Hansman et al. (2021)); shown are sample localities in Ruwi-Yiti Unit and Yenkit shear zone, axial trace of Saih Hatat fold nappe and Hercynian unconformity. Note syntectonic Muti Formation (92-86 Ma old) above rocks of Arabian platform at base of non-HP overriding plate. (b) NE-SW cross section showing overall structure of Saih Hatat window with ages of high-pressure (HP) metamorphism and metamorphism of metamorphic sole and subsequent crystallization of Samail Ophiolite. Color code: blue boxes = "cold" ~100 Ma metamorphism, pink boxes = "hot" ~100 Ma metamorphism, white box = "young" ~80 Ma HP metamorphism; ~100 Ma thrust in blue, younger thrusts, fold nappe and normal faults in black providing tectonic context.

10.1029/2022TC007531

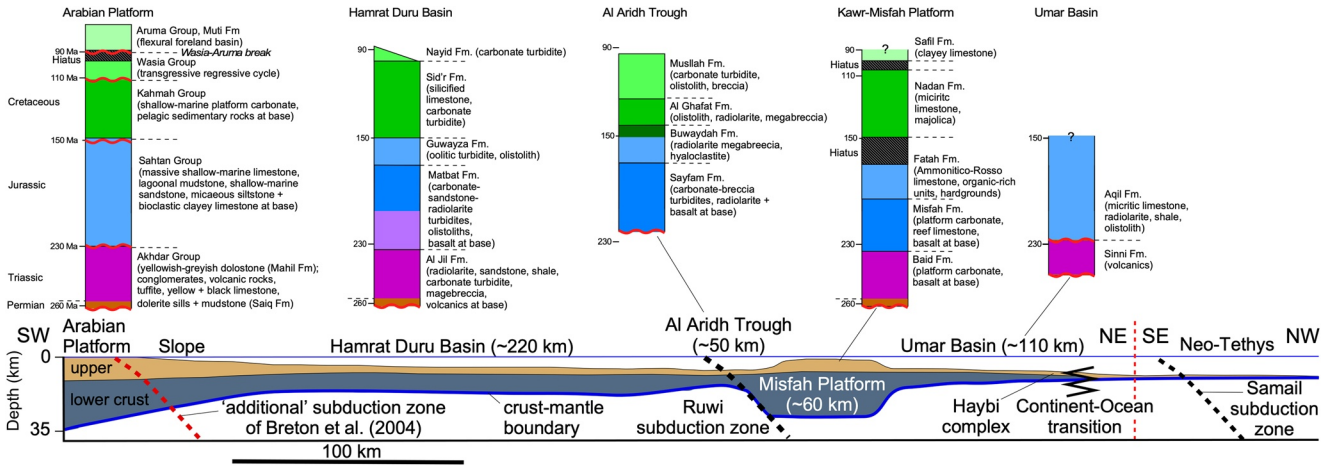

Figure 4. Mid-Cretaceous paleogeographic restoration of NE Arabian rifted margin before onset of subduction (Béchennec et al., 1990; Blechschmidt et al., 2004; Searle, 2007); margin was structured during two rifting phases in late Permian and middle/late Triassic resulting in splitting of Hawasina Basin into two basins separated by Misfah Platform; Al Aridh Trough was subjected to both rifting processes. Stratigraphic columns provide generalized succession in various segments of rifted margin (modified from Béchennec et al. (1990)). Note changing direction of rifted margin section.

the distal Umar Basin, which transitions into Triassic/Jurassic Neo-Tethyan oceanic crust (Figure 4). Both rifting events were accompanied by extensive alkaline magmatism (and the Hamrat Duru Basin was affected by both events) with mid/late Triassic MORB-type basalts near the continent-ocean transition (Searle, 2007) in the outermost Umar Basin. Shear-wave velocity data depict a mafic rifted-margin crust with abundant mafic intrusions and/or underplated lower crust (Weidle et al., 2022). The structure of the Arabian rifted margin established in the mid/late Triassic was retained until the mid-Cretaceous initiation of subduction.

Searle and Malpas (1980) and Searle (2019) referred to the distal Umar Basin as the Haybi complex. This complex is a series of imbricated rocks that include a late Cretaceous sedimentary mélange, Triassic volcanic rocks, isolated Permo-Triassic exotic limestones (<900 m thick), metamorphic rocks and serpentinites, which are above marine sediments of the Hawasina nappes and beneath the Semail Ophiolite. Searle (2019) regard the Haybi complex near the continent-ocean transition as the most likely protolith of the HP Ruwi rocks (metamorphosed under a thermal gradient of 8–10°C km^{-1}) and also of the metamorphic sole (formed under a prograde-to-peak metamorphic thermal gradient of 20–25°C km^{-1} that increased to ~30°C km^{-1} during decompression and partial melting (Ambrose et al., 2021; Garber et al., 2020; Searle & Cox, 2002)).

Other than the mainly Triassic through Cretaceous Al Aridh Trough and Umar Basin, all other parts of the Hawasina Basin have extensive Permo-Triassic platform-type carbonates with volcanic rock sequences at their base (Figure 4). At the slopes of the intervening Misfah Platform mass flows produced turbidite and megabreccia deposits in the adjacent basins. Large carbonate slices of the Misfah Platform form the "Oman Exotics." The remnants of the Al Aridh Trough occur tectonically below these Oman Exotics and above the sediments of the Hamrat Duru Basin in the central part of the Oman Mountains (Béchennec et al., 1990; Glennie et al., 1974; Searle, 2019).

The conclusion from this summary is that platform-type carbonates are not only restricted to the Arabian Platform proper, but also make up the Misfah Platform (Figure 2). The preserved remnants (mainly dolostone) of the Misfah Platform outside the Saih Hatat window are un- or very-low-grade metamorphosed. In the Saih Hatat window, these remnants are recrystallized. The Misfah Platform is supposed to have escaped subduction (Béchennec et al., 1990; Searle, 2019). For thermal reasons, the Haybi complex is unlikely to be the educt of both: the "hot" metamorphic sole and the "cold" Ruwi HP rocks.

2.1.2. Metamorphic Sole and Samail Ophiolite

Three consistent, well-defined Lu-Hf garnet-whole rock isochron ages between 105.2 and 101.9 Ma (maximum 2σ uncertainty limits) constrain prograde (~550°C/0.8 GPa) to peak (~850°C/1.1–1.3 GPa) HT metamorphism of the metamorphic sole (Guilmette et al., 2018). Subsequent partial melting during decompression of the exhuming metamorphic sole is constrained by U-Pb zircon ages of 100.4-92.5 Ma, a modeled Lu-Hf garnet-whole rock

isochron age of 93.0 ± 0.5 Ma (Garber et al., 2020), U-Pb monazite (99.7-95.3 Ma) and titanite (102.0-93.9 Ma) ages (Soret et al., 2022). Hacker et al. (1996) suggested that amphibolite-facies metamorphism and deformation was completed by ~93 Ma (Figure 3).

A plethora of detailed studies showed that the suprasubduction-zone oceanic crust of the Samail Ophiolite (e.g., MacLeod et al., 2013) formed at 96.2 to 95.0 Ma, with late-stage plagiogranite crystallizing between 95.9 and 94.0 Ma (Rioux et al., 2021; Tilton et al., 1981). Based on the interpretation of K-Ar hornblende and biotite ages from the oceanic crust as cooling ages, Hacker (1991) proposed that the Samail Ophiolite was rapidly emplaced by intraoceanic thrusting at rates of ~15 cm a^{-1}.

2.2. Saih Hatat Window

The overall architecture of the Saih Hatat HP window is complicated and different subdivisions exist (see Figure 6 in Hansman et al., 2021). We use the tectonic scheme of Agard et al. (2010) distinguishing four major HP units with the Ruwi-Yiti Unit at the top (Figures 1 and 2).

The Ruwi-Yiti Unit was emplaced above the underlying Al Khuryan-Quryat-Mayh-Saih Hatat Unit by NE-dipping shear zones, one of which is the Yenkit shear zone. The latter has an early top-to-the-SW shear sense (Searle et al., 2004). The Ruwi-Yiti and Al Khuryan-Quryat-Mayh-Saih Hatat units make up the upper plate of the HP complex and are separated from the lower plate by the top-to-the-NE displacing Upper Plate/Lower Plate Discontinuity (UP-LP) (Gregory et al., 1998; Miller et al., 1998) (note that the term "plate" refers to a series of rock units, not to tectonic plates). Semi-restorable cross sections by Hansman et al. (2021) showed that the original dip angle of the UP-LP was subhorizontal. The blueschist-facies Hulw and the eclogite-facies As Sifah units comprise the lower plate. These two units are separated from each other by the top-to-the-NE As Sheik normal shear zone, which is cut by the UP-LP (Figure 2).

The As Sifah Unit experienced HP metamorphism at 78 ± 2 Ma (El-Shazly et al., 2001) or 79 ± 1 Ma (Warren et al., 2003, 2005) (see detailed discussion in Hansman et al. (2021)). Garber et al. (2021) reported three Sm-Nd garnet-whole-rock ages between 81 ± 1 and 78 ± 2 Ma. Because the garnets have typical growth zonation, the latter ages reflect a prograde-to-peak HP stage.

The simplifying view that *all* HP units of the Saih Hatat window are 81-76 Ma in age is misleading, as the structurally higher HP units might have a pre-81-Ma HP overprint. K-Ar mica ages suggest that HP metamorphism in the Ruwi subunit already occurred at 95 ± 8 Ma (Montigny et al., 1988). The Montigny et al. (1988) study produced a number of K-Ar ages from the Saih Hatat window ranging between 239 and 58 Ma (their Figure 2). El-Shazly and Lanphere (1992) reported an $^{40}Ar/^{39}Ar$ age of 80 ± 2 Ma from a lawsonite schist of the Ruwi subunit. El-Shazly and Lanphere reported additional $^{40}Ar/^{39}Ar$ white-mica ages between 111 and 72 Ma, and El-Shazly et al. (2001) $^{40}Ar/^{39}Ar$ white-mica ages ranging from 136 to 85 Ma.

Because of the significant spread, Hacker and Gnos (1997) suggested that $^{40}Ar/^{39}Ar$ and K-Ar ages in the HP rocks are commonly compromised by excess ^{40}Ar and therefore are geologically meaningless. Warren et al. (2011) conducted a detailed $^{40}Ar/^{39}Ar$ study on HP phengite and reported ages between 132 and 66 Ma from the As Sifah Unit. Some phengite cores yielded older ages, occasionally phengite rims yielded older ages. Warren et al. (2011) concluded that "the range of $^{40}Ar/^{39}Ar$ ages measured in Oman micas are best interpreted as excess argon" and that "excess argon contamination of metamorphic white micas in HP terranes is probably the rule rather than the exception". Therefore, we do not consider K-Ar and $^{40}Ar/^{39}Ar$ ages in this work.

2.3. How Many Subduction Zones?

The intraoceanic Samail subduction zone formed in the mid-Cretaceous and the igneous oceanic rocks, which subsequently formed the Samail Ophiolite, crystallized above this subduction zone (Guilmette et al., 2018; Hacker & Gnos, 1997; Rioux et al., 2021; Searle, 2007). Many authors explain that sole metamorphism, ophiolite obduction, and the supposedly distinctly later (15–20 Ma) formation of the entire HP complex occurred by tectonic processes in this single subduction zone (Agard et al., 2020; Searle et al., 2022; Soret et al., 2022). The age break of 15–20 Ma would be in line with the envisaged timeframe for subduction-zone thermal equilibration (Lallemand & Arcay, 2021; Peacock, 1990). The missing HP metamorphism of the incoming Hawasina and Misfah platform rocks is explained by an upper-crustal decoupling horizon within the rifted-margin succession (Agard et al., 2010).

In contrast, Searle et al. (2022, their Figure 6) implied that the HP overprint of the Ruwi subunit occurred already at 96-94 Ma in the Samail subduction zone, which at that time was characterized by a thermal gradient of 30°C km^{-1}. A problem with the Searle et al. proposition is that HP metamorphism of the carpholite-lawsonite phyllite of the Ruwi subunit occurred under a thermal gradient of 8–10°C km^{-1} (Agard et al., 2010).

In contrast, El-Shazly et al. (2001) and Breton et al. (2004, their Figure 8) proposed tectonic models involving two subduction zones. Breton et al. (2004) invoked the outboard Samail intraoceanic subduction zone beneath the future Samail Ophiolite, but they also envisaged an inner, intracontinental subduction zone near the Arabian Platform (Figure 4). Breton et al. (2004) suggested that the outer Samail subduction zone formed first shortly followed by intracontinental subduction between 95 and 90 Ma.

3. Rb-Sr Ages

3.1. Rationale

For testing whether at least some of the Saih Hatat rocks may have a HP overprint >81 Ma, we sampled the uppermost HP unit (the Ruwi-Yiti Unit) and the Yenkit shear zone for Rb-Sr multimineral isochron analysis. We collected carpholite- and phengite-bearing samples from the Ruwi-Yiti Unit (see Supporting Information S1 for detailed descriptions of the samples). Previous work by Agard et al. (2010) showed that this unit experienced peak-HP metamorphism at ∼1.0 GPa and 300–330°C. We also sampled phengite-bearing carbonaceous mylonite from the Yenkit shear zone (Figure 2). The isotopic ages for HP metamorphism and associated deformation of the uppermost Ruwi-Yiti Unit will shed light on the dual "hot"-ophiolite/"cold"-HP-complex subduction-zone connection and whether "hot" and "cold" formed in one single or two separate subduction zones.

3.2. Rb-Sr Dating

The Rb-Sr multimineral dating approach mainly relies on muscovitic to phengitic white mica as a high-Rb/Sr phase. The Rb-Sr system of white mica is known to be thermally stable against diffusional reset up to temperatures >600°C (Glodny et al., 2008), whereas synkinematic recrystallization during progressive ductile deformation may lead to open system behavior, Sr-isotopic exchange with simultaneously recrystallizing phases, and age reset at temperatures as low as ∼300°C (Müller et al., 2000). In strongly sheared low- to medium grade rocks (as in the analyzed schists and mylonites of this study) the Rb/Sr age signal will, therefore, date the latest, waning stages of ductile deformation. This is when both the now-recorded metamorphic pressure-temperature conditions are frozen in, and synkinematic recrystallization of white mica and its paragenetic phases comes to an end. The grain-size sensitivity of mineral shear strengths (Platt & Behr, 2011) provides a means to test for both the presence of isotopic relics and for protracted non-penetrative deformation. White mica is analyzed in different grain-size fractions. Identical ages for all grain-size fractions testify to a clear-cut event of penetrative deformation, whereas a positive correlation between white-mica grain size and apparent ages may indicate prolonged shearing, with the apparent age for the smallest grain-size fraction being a maximum age for the end of deformation (e.g., Halama et al., 2018). A more detailed outline on the methodology along with sample descriptions are provided in Table 1 and together with analytical protocols and the rationale of the Rb-Sr data acquisition in Supporting Information S1.

3.3. Age Data

Samples OM19-1 and OM21-4 are both from strongly deformed, red/gray, calcareous phyllite. Both samples contain ∼80% white mica, as well as minor quartz, carpholite, chlorite, carbonate, and feldspar (Table 1). The Rb-Sr data for five mineral fractions from OM19-1 yield an age of 98.03 ± 0.88 Ma (mean squared weighted deviation (MSWD) = 1.4, Figure 5a). We interpret the age as dating the end of ductile shearing at HP metamorphic conditions (i.e., as dating the freezing-in of the current carpholite-bearing HP assemblage). A six-point isochron of sample OM2-14 provides an age of 97.04 ± 0.76 Ma (MSWD = 2.0, Figure 5b). Within the margins of uncertainty, this age is indistinguishable from the one obtained from OM19-1 and is interpreted in the same way.

Samples OM21-3 and OM21-2 are mylonitic calcschists from the Yenkit shear zone (Figure 2, Table 1). All samples contain calcite and white mica, with minor chlorite, quartz and hematite. The Rb-Sr data for OM21-3

Table 1
Characterization of Dated Rock Samples

Sample GPS data	Rock type	Fabric	Assemblage	Comments	Interpretation of age data
Ruwi-Yiti					
OM19-1 23°34′30″, 58°32′58″	Carpholite-bearing phyllite	Reddish, fine-grained, tightly foliated, phyllitic schist, distinct foliation, top-NE shear sense	White mica (~90%) quartz, chlorite, carbonate (mainly calcite), minor albite, oxide phases, carpholite	No post-high-P alteration	Top-NE shearing at high-P metamorphism
OM21-4 23°35′39″, 58°32′29″	Carpholite-bearing phyllite	Gray to reddish fine-grained, tightly foliated phyllitic mylonite with hematite aggregates	White mica (~90%) quartz, chlorite, calcite (orange), minor albite, apatite, hematite pseudomorphs after pyrite	No post-high-P alteration	Top-NE shearing at high-P metamorphism
OM21-2 23°31′06″, 58°42′19″	Calcschist (Yenkit shear zone)	Fine grained, mylonitic	Calcite (partly colorless/white, partly yellowish), white mica, and accessory apatite	Isotopically homogeneous calcite population, positive correlation between white-mica apparent age and grain size	Prolonged mylonitization
OM21-3 23°31′03″, 58°42′19″	Calcschist (Yenkit shear zone)	Fine grained, mylonitic	Calcite (partly colorless/white, partly yellowish), white mica	n/a	Mylonitization

show differences between large (≥160–355 μm) and small (<160 μm) white mica. Five mineral fractions of sample OM21-3 give an age of 99.6 ± 3.7 Ma (MSWD = 3.5, Figure 5c). The white-mica grain-size fraction >200 μm plots slightly above the regression line. This indicates minute Sr-isotopic inhomogeneities in the white-mica population. The age information is internally overdetermined as all three analyzed white-mica fractions provide ages near 100 Ma. Therefore, we confidently interpret the age 99.6 ± 3.7 Ma to reflect the end of mylonitization.

Sample OM21-2 provided a six-point regression line corresponding to an age of 98.5 ± 7.4 Ma (MSWD = 18, Figure 5d). The elevated MSWD is related to slight disequilibria within the white-mica population. It appears that there is a minor but significant positive correlation between white-mica apparent ages and grain size. When calculated with calcite (the dominant reservoir of Sr in the rock) apparent ages range between 102.7 ± 1.5 Ma (white mica >200 μm) and 94.5 ± 1.4 Ma (white mica 90–63 μm). We interpret this pattern to reflect either a prolonged episode of deformation during mylonitization, or partial reworking of an assemblage with an age >102.7 ± 1.5 Ma during a deformation event at ≤94.5 ± 1.4 Ma.

3.4. Summary and Interpretation of Rb-Sr Age Data

Our data for HP metamorphism provide consistent and reproducible ages of 98.9-96.3 Ma (maximum 2σ uncertainty limits) for the end of ductile deformation at HP metamorphic conditions of the Ruwi subunit. The age information of the two samples from the Yenkit shear zone is mixed. Sample OM21-3 provides a robust age of ~100 Ma for the end of mylonitization, which is corroborated by the apparent age of 102.7 ± 1.5 Ma from sample OM21-2. The apparent age of 94.5 ± 1.4 Ma for the finest white-mica population (90-63 μm) of sample OM21-2 indicates reworking of the Yenkit shear zone and supporting long lasting deformation between ≥104 and 93 Ma (Figure 3). Our interpretation of the four ages is that the Yenkit shear zone facilitated early underthrusting, starting at ~104 Ma, causing HP metamorphism, which ceased at 99-96 Ma. Deformation in the Yenkit shear zone continued until ~93 Ma.

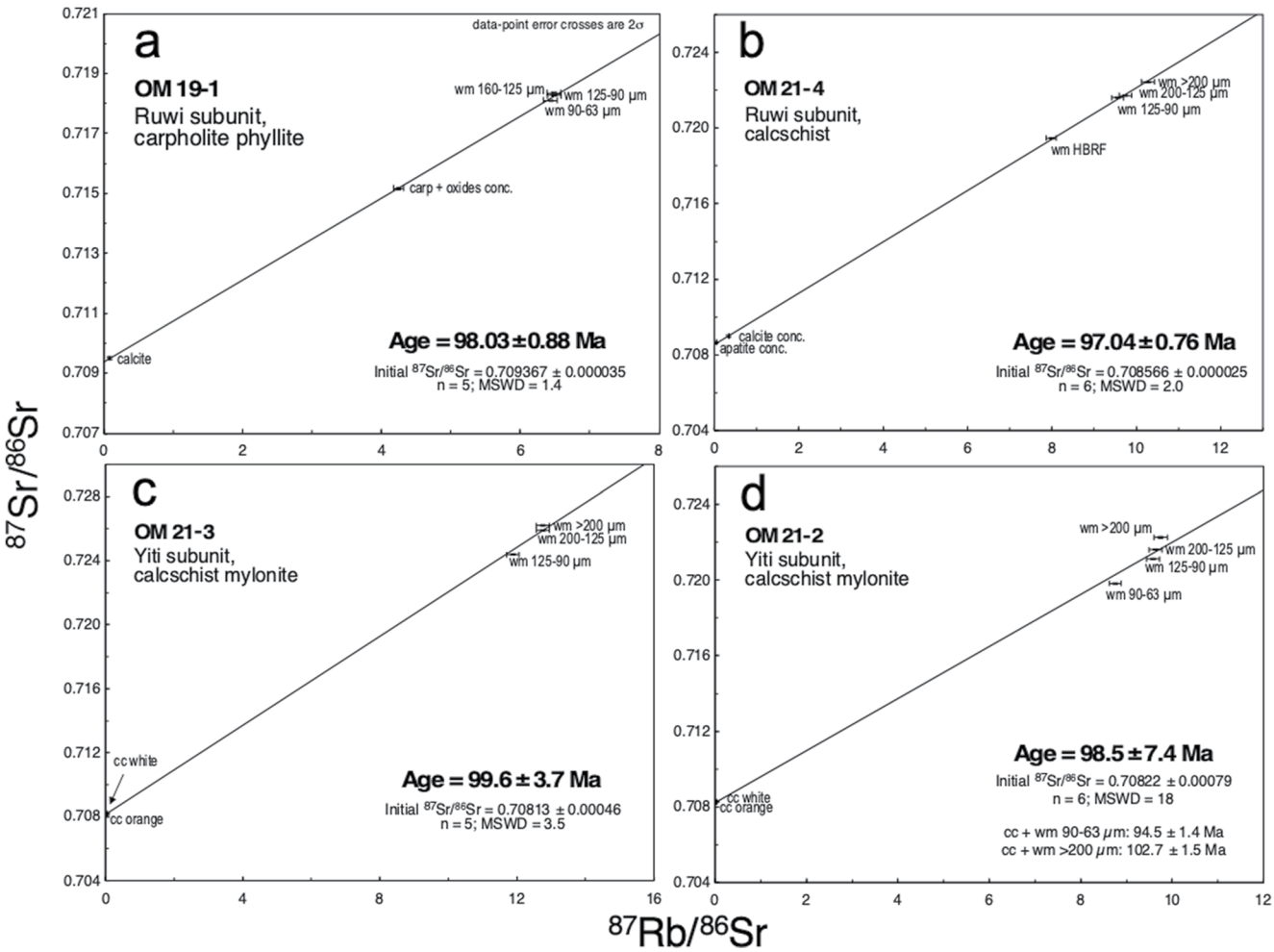

Figure 5. Rb-Sr data. (a and b) HP rocks from Ruwi subunit. (c and d) Mylonitic calcschists from Yenkit shear zone.

4. Discussion

4.1. Two Subduction Zones at Arabian Margin

Our ages of 98.9 to 96.3 Ma for late stages of HP metamorphism and deformation in the Ruwi subunit are: (a) ~3–9 Ma younger than prograde to peak metamorphism of the metamorphic sole which occurred at 105.2-101.9 Ma (Guilmette et al., 2018) (*note*: our Rb-Sr ages reflect late stages of HP processes, the early stages of which might potentially be as old or even older than metamorphism of the metamorphic sole). (b) The Rb-Sr ages are broadly coeval with partial melting of the metamorphic sole during decompression and exhumation at 100.4-92.4 Ma (Garber et al., 2020) (Figure 3). Deformation ages of up to 104 Ma indicate that the Yenkit shear zone and initial underthrusting of the metamorphic sole at the Samail subduction zone were about coeval.

Temperatures during the early stages of subduction are usually hotter than during steady-state subduction (e.g., Lallemand & Arcay, 2021; Peacock, 1990). These thermal considerations, as well as ages of <99 Ma (that date waning HP metamorphism), show that initial underthrusting in the Ruwi subduction zone may have already started by ~110 Ma (or before). This would be earlier than the inception of the Samail subduction zone. The youngest permissible age of ~93 Ma for the Yenkit shear zone overlaps with thrusting along the base of the Samail Ophiolite (Figure 2).

This discussion demands that our ages cannot be reconciled with one single subduction zone explaining Cretaceous tectonics at the Arabian convergent margin. The key issue is that the processes during and after the initiation of the Samail subduction zone, and subsequent melting of the sole, occurred under a thermal gradient of

20–25°C km^{-1} at 105-102 Ma, which then increased to 30°C km^{-1} between 100 and 93 Ma in an infant, thermally transient, hot subduction zone. Our Rb-Sr HP ages of 99-96 Ma are coeval with melting of the sole and occurred in a thermally stable, steady-state subduction zone under a thermal gradient of 8–10°C/km. Therefore, it is inescapable to conclude that there must have been two subduction zones at the mid-Cretaceous Arabian margin. More importantly, we propose that the subduction zone in which the Ruwi HP rocks formed was the first to develop (Figure 6a). This is because the pressure-temperature conditions recorded in the Ruwi-Yiti HP rocks indicate thermally fully equilibrated, steady state subduction, which is in line with early underthrusting at the Yenkit shear zone at ∼104 Ma (Figure 6b). In contrast, melting processes were still occurring at 100.4-92.4 Ma in the Samail subduction zone, attesting to non-steady-state conditions and a younger age of the Samail subduction zone. The "hot" processes in the outboard Samail subduction zone were largely coeval with "cold" HP metamorphism in the thermally mature subduction zone that formed the Ruwi HP rocks, rendering the "conundrum of Samail" redundant.

We name the older subduction zone the "Ruwi subduction zone". Where would it have formed? Because continental rocks make up the Ruwi-Yiti Unit and all HP units are structurally below the Samail Ophiolite, the Ruwi subduction zone must have formed closer to the Arabian margin than the Samail Ophiolite (Figure 1b). Breton et al. (2004) proposed that the subduction zone developed at the platform margin (Figure 4), which we consider unlikely. This is because it would (a) be easier to form an intracontinental subduction zone within the strongly thinned crustal segments of the Hawasina Basin; and (b) the platform units were HP metamorphosed during the second, well-known pulse of HP metamorphism at 81-76 Ma, but the problem is to explain the ≥99-96 Ma HP metamorphism of the Ruwi subunit. We consider it most likely that Ruwi subduction localized in the dense, mafic-magma-rich and thinned (attenuated by two rifting processes) crust of the Al Aridh Trough (see below). In this case, the Ruwi rocks would be derived from the Al Aridh Trough and were underthrust beneath the Misfah Platform (Figure 6).

4.2. Ruwi Subduction Zone

Gray and Gregory (2004) and Searle et al. (2004) argued that buoyant continental crust could not be subducted to depths of ∼80 km unless a significant amount of leading oceanic slab dragged it down. However, subduction is triggered by gravitational instability (Turcotte and Schubert, 2022). Stüwe and Schuster (2010) showed that regions of thin continental crust and thick mantle lithosphere can be negatively buoyant. An example for this are the Mediterranean orogens, which are characterized by a number of intracontinental subduction zones, the formation of which were aided by the heavy lithosphere of the Adria microcontinent (Ring et al., 2010). Poupinet et al. (2002) suggested that subduction of the mantle part of the lithosphere in the interior of the Asian Plate formed the Tien Shan intracontinental mountain range. In general, continental lithosphere is older, colder, and thus can be heavier than oceanic lithosphere (Jaupart & Mareschal, 2015; Stüwe & Schuster, 2010).

The Arabian rifted margin was substantially thinned during two Permian-Triassic rifting events and is made up by highly attenuated crust underlain by thermally thickened (and relatively negatively buoyant) mantle lithosphere. The subducted lithosphere was contaminated/underplated by dense mafic rocks, which increased its density (Weidle et al., 2022). Subsequently, extension was partitioned into the oceanic domain of Neotethys and the continental lithosphere of the rifted margin started to cool. Passive thermal equilibration (i.e., thickening) of the heavy lithospheric mantle causes subsidence (Holt et al., 2010), which at the Arabian margin resulted in the formation of the Hamrat-Duru Basin (Figure 4). We suggest that the transition from negative to positive vertical buoyancy occurs near the Arabian Platform, which was not extended and hence had normal crustal thickness.

We consider it mechanically plausible that the onset of subduction at the Arabian rifted margin was due to a gravitational instability provided by a prolonged cooling phase following Permo-Triassic rifting. Subduction commenced at a locus of extreme strength contrast between the Al Aridh Basin and the Misfah Platform, the latter of which was not affected by Permo-Triassic extension and therefore had normal crustal thickness and a relatively light lithospheric mantle.

4.3. Subduction and Obduction

Figure 6 shows our interpretation of the tectonic evolution of the two subduction zones at the Arabian margin, largely based on the plate-tectonic reconstructions of van Hinsbergen et al. (2019, 2021). Van Hinsbergen

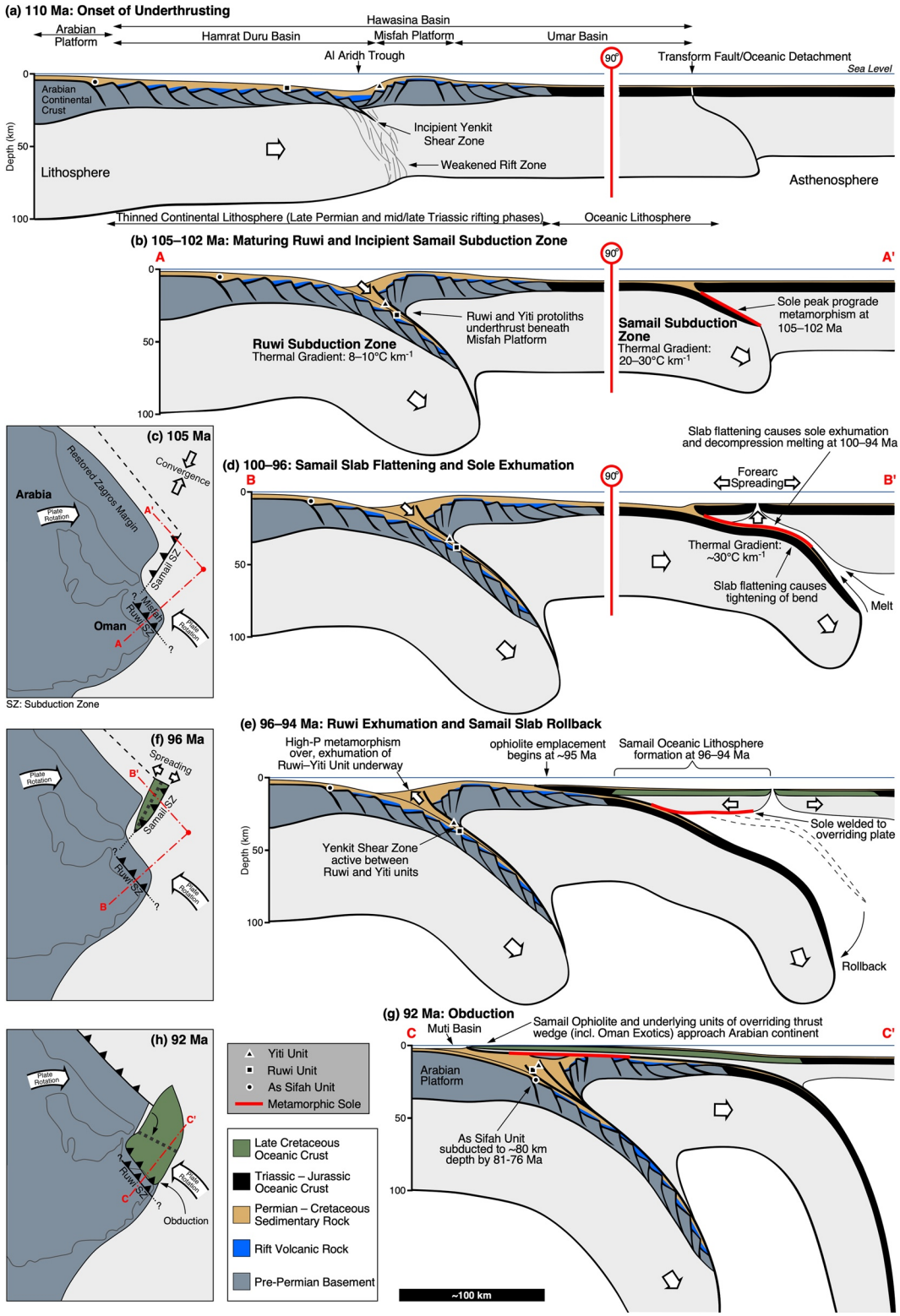

Figure 6.

et al. (2021) shows two competing processes, one would be NNE-directed Neotethys spreading and plate convergence; the second process plume-induced clockwise plate rotation of Arabia resulting in a component of ~E-W convergence. These two directions are subperpendicular to the intra-Neo-Tethys trench-transform system (Figure 1b). Plate convergence in the Arabian sector of Neo-Tethys was first accommodated by subduction along a proto-Zagros/Makran subduction system by 130 Ma (Burg, 2018) and initial convergence rates were ~2–3 cm a^{-1}. The convergence rates increased to ~5–6 cm a^{-1} after ~118 Ma (Müller et al., 1997). We envisage that the increase in NNE-directed convergence rates triggered Ruwi subduction along an ENE-striking segment of the intra-Neotethys trench-transform system (Figure 1b) sometime after 118 Ma.

Van Hinsbergen et al. (2021) argued that the formation of the Morondava plume controlled Madagascar-India continental break-up and exerted clockwise rotation of Africa/Arabia and counter-clockwise rotation of India. This was a potential driver of Samail subduction initiation. The exact timing when the rising plume caused the plate rotations is not known. An important phase of transform rifting was initiated at ~100 Ma (Plummer & Belle, 1995). We envisage that plume-induced E-W convergence triggered Samail subduction along the N-S-striking segments of the intra-Neotethys trench-transform system by 105 Ma (Figures 1b and 6b). The Ruwi and Samail subduction zones were almost perpendicular to each other at this stage.

The next important step would be the melting of the metamorphic sole and the formation of the Samail Ophiolite. Van Hinsbergen et al. (2015) and Ambrose et al. (2021) proposed that exhumation of the metamorphic sole was accomplished by attenuation of the mantle wedge above a shallowing subducting slab (Figure 6d). Slab shallowing remains the only plausible option for sole exhumation. This is because there is no field evidence that a normal fault above the metamorphic sole aided its exhumation. In addition, the upper plate needs to thin during sole exhumation and melting, a process that would lower the subduction angle and increase frictional forces between the tectonic plates (Espurt et al., 2008), slowing down Samail subduction.

Nonetheless, slab shallowing does not explain the high supra-subduction spreading rates of 10–20 cm a^{-1} as inferred from the U-Pb zircon ages of dikes from the Samail Ophiolite (Rioux et al., 2021). These spreading rates are distinctly greater than the plate motion rates of Arabia (Müller et al., 1997). The only likely option to achieve the fast spreading rates appears to be slab rollback. Initiation of subduction rollback requires about 100–150 km of forced subduction, after which the negative buoyancy of the tip of the subducted slab leads to enhanced slab sinking triggering rollback (Becker et al., 1999; Chertova, 2014; Gurnis et al., 2004). Leng and Gurnis (2011) proposed that slab sinking causes a strong influx of asthenosphere above the foundering slab (Figure 6d). This rollback must have followed initial melting of the sole by 100 Ma (Garber et al., 2021) and subsequently caused fast spreading forming the Samail Ophiolite at 96-94 Ma. Rollback probably aided the clockwise rotation of the Samail subduction zone as indicated by paleomagnetic data (Morris et al., 2016; van Hinsbergen et al., 2019).

The significant high of the Misfah Platform (e.g., Blechschmidt et al., 2004) would have approached the Samail subduction zone at sometime near 95-93 Ma (depending on subduction rates, which are unknown) (Figure 6e). The incoming Misfah Platform would most likely have caused a reduction in wedge taper (Davis et al., 1983) forcing the subduction thrust to step back and override the incoming bathymetric high of the platform, causing out-of-sequence thrusting. A reduction in wedge taper would also cause additional shortening across the subduction wedge, which might be needed to explain, or would have aided, the high displacement rates of ~15 cm a^{-1} of the Samail Ophiolite (Hacker et al., 1996).

Figure 6. Subduction-zone evolution at Arabian rifted margin featuring underthrusting of Al Aridh Trough under Misfah Platform and subsequent Samail subduction zone. (a) Simplified cross section of Arabian margin at 110 Ma at envisaged onset of Ruwi subduction zone. Incipient underthrusting of strongly thinned, mafic-rich and dense crust and thermally thickened lithospheric mantle of Al Aridh Trough underneath buoyant Misfah Platform; Yiti subunit derived from extended and thinned southern margin of Misfah Platform and was plucked off by subduction erosion. (b) Incipient formation of Samail subduction zone and prograde high-T metamorphism of metamorphic sole at 105-102 Ma (Guilmette et al., 2018) while Ruwi subduction zone thermally equilibrating; note vastly different thermal gradients. Map view of cross section shown in (b) highlighting different orientation of subduction zones and convergence direction within Arabian Neotethys and plume-induced rotation of Arabian Plate. (d) Advanced stage at ~100–96 Ma showing decompressional melting of metamorphic sole at thermal gradient of 30°C km^{-1}; advanced subduction and incipient exhumation of cold Ruwi-Yiti high-pressure rocks. (e) Samail oceanic lithosphere crystallizing, exhuming metamorphic sole welded to base of ophiolite and both started to override sediments of Umar Basin; Misfah Platform envisaged to enter Samail subduction zone at about this stage, bathymetric high reduced wedge taper causing increased shortening across Samail subduction zone aiding or triggering rapid movement of Samail Ophiolite at rates of 15 cm a^{-1} (Hacker, 1991) toward Arabian margin. Ruwi-Yiti Unit exhumes. (f) Map view of initial spreading of Samail Ophiolite. (g), (h) At ~92 Ma, Samail Ophiolite approached Arabian Platform and Muti foreland basin sediments accumulate; overriding-plate thrust wedge composed in descending order by Samail Ophiolite with metamorphic sole, Umar section of Hawasina nappes, Oman Exotics (i.e., carbonates of Misfah Platform) and Hamrat-Duru section of Hawasina nappes (compare to Figure 4). Note unknown subduction rates leaving exact tempospatial aspects speculative. (c, f, and h) modified from van Hinsbergen et al. (2019, 2021).

The buoyant lithosphere of the incoming Misfah Platform may have made continued subduction at the Samail subduction zone difficult. Plate convergence was distinctly easier to absorb at the (thinned by rifting) inboard, intracontinental Ruwi subduction zone. Accordingly, the 81–76 Ma HP rocks of the lower parts of the Saih Hatat complex would have formed at the inboard, stable, steady-state subduction zone. Such a proposition is also geometrically simpler (Figure 6). If the Samail subduction zone had survived, the rocks that formed and were accreted in the Ruwi subduction zone should have been (re)subducted a second time by the Samail subduction zone, for which there is no evidence.

5. Concluding Remarks

New Rb-Sr multimineral ages for HP metamorphism and deformation of the Ruwi-Yiti Unit of the Saih Hatat window demand the existence of two subduction zones at the mid-Cretaceous Arabian rifted margin, and provides a refined solution of the "conundrum of Samail." At 105-93 Ma, the thermal structure of the infant, outboard Samail subduction zone was not equilibrated, while the inboard, intracontinental Ruwi subduction zone had a distinctly different, fully thermally equilibrated thermal structure. These contrasting thermal conditions, along with ages of up to ∼104 Ma for the Yenkit shear zone, suggest that the Ruwi subduction zone was the first to develop at the Arabian margin. The docking of the Misfah Platform made sustained underthrusting at the Samail subduction zone difficult. It appears more likely that ongoing convergence, and the prominent Saih Hatat HP metamorphism at 81-76 Ma, was accomplished by the Ruwi subduction zone.

Data Availability Statement

All data used in this manuscript are cited in the text and tables or can be found at https://doi.org/10.17045/sthl-muni.20455470.v1.

Acknowledgments
Funded by the Swedish Science Council (VR Grant 2021-04075). We thank Douwe van Hinsbergen and an anonymous reviewer for comments and the Associate Editor for guidance. We also acknowledge email conversations with Douwe van Hinsbergen on slab rollback and rotation of the Samail subduction zone.

References

Agard, P., Prigent, C., Soret, M., Dubacq, B., Guillot, S., & Deldicque, D. (2020). Slabitization: Mechanisms controlling subduction development and viscous coupling. *Earth-Science Reviews*, *208*, 103259. https://doi.org/10.1016/j.earscirev.2020.103259

Agard, P., Searle, M. P., Alsop, G. I., & Dubacq, B. (2010). Crustal stacking and expulsion tectonics during continental subduction: P-T deformation constraints from Oman. *Tectonics*, *29*(5), 1–19. https://doi.org/10.1029/2010TC002669

Aldega, L., Carminati, E., Scharf, A., & Mattern, F. (2021). Thermal maturity of the Hawasina units and origin of the Batinah Mélange (Oman Mountains): Insights from clay minerals. *Marine and Petroleum Geology*, *133*, 105316. https://doi.org/10.1016/j.marpetgeo.2021.105316

Aldega, L., Carminati, E., Scharf, A., Mattern, F., & Al-Wardi, M. (2017). Estimating original thickness and extent of the Semail Ophiolite in the eastern Oman Mountains by paleothermal indicators. *Marine and Petroleum Geology*, *84*, 18–33. https://doi.org/10.1016/j.marpetgeo.2017.03.024

Ambrose, T. K., Waters, D. J., Searle, M. P., Gopon, P., & Forshaw, J. B. (2021). Burial, accretion, and exhumation of the metamorphic sole of the Oman-UAE ophiolite. *Tectonics*, *40*(4), e2020TC006392. https://doi.org/10.1029/2020TC006392

Béchennec, F., Le Métour, J., Rabu, D., Bourdillon-de-Grissac, C., de Wever, P., Beurrier, M., & Villey, M. (1990). The Hawasina Nappes; Stratigraphy, paleogeography and structural evolution of a fragment of the South-Tethyan passive continental margin. In A. H. F. Robertson, M. P. Searle, & A. C. Ries (Eds.), *The geology and tectonics of the Oman region* (Vol. 49, pp. 213–223). https://doi.org/10.1144/GSL.SP.1992.049.01.14

Béchennec, F., Roger, J., Le Metour, J., & Wyns, R. (1992). *Geological map of Seeb, sheet NF40-03 1:250,000*. Sultanat of Oman, Ministry of Petroleum and Minerals.

Becker, T. W., Faccenna, C., O'Connell, R. J., & Giardini, D. (1999). The development of slabs in the upper mantle: Insights from numerical and laboratory experiments. *Journal of Geophysical Research*, *104*(B7), 15207–15226. https://doi.org/10.1029/1999jb900140

Blechschmidt, I., Dumitrica, P., Mater, A., Krystyn, L., & Peters, T. (2004). Stratigraphic architecture of the northern Oman continental margin-Mesozoic Hamrat Duru Group, Hawasina complex, Oman. *GeoArabia*, *9*(2), 81–132. https://doi.org/10.2113/geoarabia090281

Breton, J. P., Bechennec, F., Le Metour, J., Moen-Maurel, L., & Razin, P. (2004). Eoalpine (Cretaceous) evolution of the Oman Tethyan continental margin: Insights from a structural field study in Jabal Akhdar (Oman Mountains). *GeoArabia*, *9*(2), 41–58. https://doi.org/10.2113/geoarabia090241

Burg, J.-P. (2018). Geology of the onshore Makran accretionary wedge: Synthesis and tectonic interpretation. *Earth-Science Reviews*, *185*, 1210–1231. https://doi.org/10.1016/j.earscirev.2018.09.011

Chertova, M. (2014). 3-D subduction modeling, western Mediterranean, absolute plate motion, tectonic reconstruction, Rif-Betic, open boundaries. *Utrecht Studies in Earth Sciences*, *68*. ISBN: 9789062663774.

Cowan, R. J., Searle, M. P., & Waters, D. J. (2014). Structure of the metamorphic sole to the Oman ophiolite, Sumeini window and Wadi Tayyin: Implications for ophiolite obduction processes. *Geological Society*, *392*(1), 155–175. https://doi.org/10.1144/sp392.8

Davis, D., Suppe, J., & Dahlen, F. A. (1983). The mechanics of fold-and-thrust belts and accretionary wedges. *Journal of Geophysical Research*, *88*, 1153–1172. https://doi.org/10.1029/JB088iB02p01153

Dewey, J. F., & Bird, J. (1971). Origin and emplacement of the ophiolite suite: Appalachian ophiolites in Newfoundland. *Journal of Geophysical Research*, *76*(14), 2120–2121. https://doi.org/10.1139/f70-24010.1029/jb076i014p03179

El-Shazly, A. K., Bröcker, M., Hacker, B., & Calvert, A. (2001). Formation and exhumation of Blueschists and Eclogites from NE Oman: New perspectives from Rb–Sr and $^{40}Ar/^{39}Ar$ dating. *Journal of Metamorphic Geology*, *19*(3), 233–248. https://doi.org/10.1046/j.1525-1314.2001.00309.x

El-Shazly, A. K., & Lanphere, M. A. (1992). Two high pressure metamorphic events in NE Oman: Evidence from $^{40}Ar/^{39}Ar$ dating and petrological data. *The Journal of Geology*, *100*(6), 731–751. https://doi.org/10.1086/629625

Espurt, N., Funiciello, F., Martinod, J., Guillaume, B., Regard, V., Faccenna, C., & Brusset, S. (2008). Flat subduction dynamics and deformation of the South American plate: Insights from analog modeling. *Tectonics*, *27*(3), TC3011. https://doi.org/10.1029/2007TC002175

Garber, J. M., Rioux, M., Kylander-Clark, A. R. C., Hacker, B. R., Vervoort, J. D., & Searle, M. P. (2020). Petrochronology of Wadi Tayin metamorphic sole metasediment, with implications for the thermal and tectonic evolution of the Samail Ophiolite (Oman/UAE). *Tectonics*, *39*(12). https://doi.org/10.1029/2020TC006135

Garber, J. M., Rioux, M., Searle, M. P., Kylander-Clark, A. R. C., Hacker, B. R., Vervoort, J. D., et al. (2021). Dating continental subduction beneath the Samail Ophiolite: Garnet, zircon, and rutile petrochronology of the as Sifah eclogites, NE Oman. *Journal of Geophysical Research: Solid Earth*, *126*(12), e2021JB022715. https://doi.org/10.1029/2021JB022715

Glennie, K. W., Boeuf, M. G. A., Hughes-Clarke, M. W., Moody-Stuart, M., Pilaar, W. F. H., & Reinhardt, B. M. (1974). *Geology of the Oman Mountains, Verhandelingen Koninklijk Nederlands Geologisch Mijnbouwkundidg*. Genootschap.

Glodny, J., Kühn, A., & Austrheim, H. (2008). Geochronology of fluid-induced eclogite and amphibolite facies metamorphic reactions in a subduction–collision system, Bergen Arcs, Norway. *Contributions to Mineralogy and Petrology*, *156*(1), 27–48. https://doi.org/10.1007/s00410-007-0272-y

Glodny, J., & Ring, U. (2022). The Cycladic Blueschist Unit of the Hellenic subduction orogen: Protracted high-pressure metamorphism, decompression and reimbrication of a diachronous nappe stack. *Earth-Science Reviews*, *224*, 103883. https://doi.org/10.1016/j.earscirev.2021.103883

Goscombe, B., Foster, D. A., Gray, D., Kelsey, D., & Wade, B. (2020). Metamorphic response within different subduction–obduction settings preserved on the NE Arabian margin. *Gondwana Research*, *83*, 298–371. https://doi.org/10.1016/j.gr.2020.02.002

Gray, D. R., & Gregory, R. T. (2004). Comment on "Eoalpine (Cretaceous) evolution of the Oman Tethyan continental margin: Insights from a structural field study in Jabal Akhdar (Oman Mountains) by Jean-Paul Breton et al.". *GeoArabia*, *9*(4), 143–147. https://doi.org/10.2113/geoarabia0904143

Gregory, R. T., Gray, D. R., & Miller, J. M. (1998). Tectonics of the Arabian margin associated with the formation and exhumation of high-pressure rocks, Sultanate of Oman. *Tectonics*, *17*(5), 657–670. https://doi.org/10.1029/98TC02206

Guilmette, C., Smit, M. A., van Hinsbergen, D. J. J., Gürer, D., Corfu, F., Charette, B., et al. (2018). Forced subduction initiation. *Nature Geoscience*, *4907*. https://doi.org/10.1029/JB095iB04p04895

Gurnis, M., Hall, C., & Lavier, L. (2004). Evolving force balance during incipient subduction. *Geochemistry, Geophysics, Geosystems*, *5*(7), Q07001. https://doi.org/10.1029/02003GC000681

Hacker, B. R. (1991). The role of deformation in the formation of metamorphic gradients: Ridge subduction beneath the Oman ophiolite. *Tectonics*, *10*(2), 455–473. https://doi.org/10.1029/90TC02779

Hacker, B. R., & Gnos, E. (1997). The conundrum of Samail: Explaining the metamorphic history. *Tectonophysics*, *279*(1–4), 215–226. https://doi.org/10.1016/s0040-1951(97)00114-5

Hacker, B. R., Mosenfelder, J. L., & Gnos, E. (1996). Rapid emplacement of the Oman ophiolite: Thermal and geochronologic constraints. *Tectonics*, *15*(6), 1230–1247. https://doi.org/10.1029/96TC01973

Halama, R., Glodny, J., Konrad-Schmolke, M., & Sudo, M. (2018). Rb-Sr and in situ $^{40}Ar/^{39}Ar$ dating of exhumation-related shearing and fluid-induced recrystallization in the Sesia zone (Western Alps, Italy). *Geosphere*, *14*(4), 1425–1450. https://doi.org/10.1130/ges01521.1

Hansman, R. J., Ring, U., Scharf, A., Glodny, J., & Wan, B. (2021). Structural architecture and Late Cretaceous exhumation history of the Saih Hatat Dome (Oman), a review based on existing data and semi-restorable cross-sections. *Earth-Science Reviews*, *217*, 103595. https://doi.org/10.1016/j.earscirev.2021.103595

Holt, P. J., Allen, M. B., van Hunen, J., & Bjørnseth, H. M. (2010). Lithospheric cooling and thickening as a basin forming mechanism. *Tectonophysics*, *495*(3–4), 184–194. https://doi.org/10.1016/j.tecto.2010.09.014

Jaupart, C., & Mareschal, J.-C. (2015). Heat flow and thermal structure of the lithosphere. *Treatise on Geophysics*, *6*, 217–253.

Lallemand, S., & Arcay, D. (2021). Subduction initiation from the earliest stages to self-sustained subduction: Insights from the analysis of 70 Cenozoic sites. *Earth-Science Reviews*, *221*, 103779. https://doi.org/10.1016/j.earscirev.2021.103779

Le Métour, J., De Gramont, X., & Villey, M. (1986). *Geological map of Quryat sheet NF40-4D scale 1:100,000*. Directorate General of Minerals, Oman Ministry of Petroleum and Minerals.

Le Métour, J., De Gramont, X., Villey, M., & Beurrier, M. (1986). *Geological map of Masqat sheet NF40-4A scale 1:100,000 and explanatory notes*. Directorate General of Minerals, Oman Ministry of Petroleum and Minerals.

Leng, W., & Gurnis, M. (2011). Dynamics of subduction initiation with different evolutionary pathways. *Geochemistry, Geophysics, Geosystems*, *12*, Q12018. https://doi.org/10.1029/12011GC003877

Liu, F. L., Gerdes, A., & Xue, H. M. (2009). Differential subduction and exhumation of crustal slices in the Sulu HP-UHP metamorphic terrane: Insights from mineral inclusions, trace elements, U-Pb and Lu-Hf isotope analyses of zircon in orthogneiss. *Journal of Metamorphic Geology*, *27*(9), 805–825. https://doi.org/10.1111/j.1525-1314.2009.00833.x

MacLeod, C. J., Lissenberg, J. C., & Bibby, L. E. (2013). "Moist MORB" axial magmatism in the Oman ophiolite: The evidence against a mid-ocean ridge origin. *Geology*, *41*(4), 459–462. https://doi.org/10.1130/g33904.1

Miller, J. M., Gray, D. R., & Gregory, R. T. (1998). Exhumation of high-pressure rocks in northeastern Oman. *Geology*, *26*(3), 235–238. https://doi.org/10.1130/0091-7613(1998)026<0235:EOHIGH-PRI>2.3.CO;2

Montigny, R., Le Mer, O., Thuizat, R., & Whitechi, H. (1988). K–Ar and $^{40}Ar/^{39}Ar$ study of metamorphic rocks associated with the Oman ophiolite: Tectonic implications. *Tectonophysics*, *151*(1–4), 345–362. https://doi.org/10.1016/0040-1951(88)90252-1

Morris, A., Meyer, M., Anderson, M. W., & MacLeod, C. J. (2016). Clockwise rotation of the entire Oman ophiolite occurred in a suprasubduction zone setting. *Geology*, *44*(12), 1055–1058. https://doi.org/10.1130/g38380.1

Müller, R. D., Roest, W. R., Royer, J.-Y., Gahagan, L. M., & Sclater, J. G. (1997). Digital isochrons of the world's ocean floor. *Journal of Geophysical Research*, *102*(B2), 3211–3214. https://doi.org/10.1029/96jb01781

Müller, W., Mancktelow, N. S., & Meier, M. (2000). Rb-Sr microchrons of synkinematic mica in mylonites: An example from the DAV fault of the Eastern Alps. *Earth and Planetary Science Letters*, *180*(3–4), 385–397. https://doi.org/10.1016/s0012-821x(00)00167-9

Peacock, S. M. (1990). Numerical simulation of metamorphic pressure–temperature–time paths and fluid production in subducting slabs. *Tectonics*, *9*(5), 1197–1211. https://doi.org/10.1029/tc009i005p01197

Platt, J. P., & Behr, W. M. (2011). Grainsize evolution in ductile shear zones: Implications for strain localization and the strength of the lithosphere. *Journal of Structural Geology*, *33*(4), 537–550. https://doi.org/10.1016/j.jsg.2011.01.018

Plummer, P. h. S., & Belle, E. R. (1995). Mesozoic tectono-stratigraphic evolution of the Seychelles micro-continent. *Sedimentary Geology*, *96*(1–2), 73–91. https://doi.org/10.1016/0037-0738(94)00127-g

Poupinet, G., Avouac, J. P., Jiang, M., Wei, S., Kissling, E., Herquel, G., et al. (2002). Intracontinental subduction and Paleozoic inheritance of the lithosphere suggested by a teleseismic experiment across the Chinese Tien Shan. *Terra Nova*, *14*(1), 18–24. https://doi.org/10.1046/j.1365-3121.2002.00391.x

Ring, U., Glodny, J., Will, T., & Thomson, S. (2010). The Hellenic subduction system: High- pressure metamorphism, exhumation, normal faulting, and large-scale extension. *Annual Review of Earth and Planetary Sciences*, *38*(1), 45–76. https://doi.org/10.1146/annurev.earth.050708.170910

Ring, U., & Layer, P. W. (2003). High-pressure metamorphism in the Aegean, eastern Mediterranean: Underplating and exhumation from the late Cretaceous until the Miocene to recent above the retreating Hellenic subduction zone. *Tectonics*, *22*(3), 23. https://doi.org/10.1029/2001TC001350

Rioux, M., Garber, J. M., Searle, M., Kelemen, P., Miyashita, S., Adachi, Y., & Bowring, S. (2021). High-precision U-Pb zircon dating of late magmatism in the Samail ophiolite: A record of subduction initiation. *Journal of Geophysical Research: Solid Earth*, *126*(5), e2020JB020758. https://doi.org/10.1029/2020JB020758

Scharf, A., Mattern, F., Al-Wardi, M., Frijia, G., Moraetis, D., Pracejus, B., et al. (2021). The geology and tectonics of the Jabal Akhdar and Saih Hatat domes, Oman Mountains. *Geological Society of London Memoirs M54*, 1–125. https://doi.org/10.1144/M54

Searle, M. (2019). Geology of the Oman Mountains, Eastern Arabia. *Tectonophysics*.

Searle, M., Rioux, M., & Garber, J. M. (2022). One line on the map: A review of the geological history of the Semail thrust, Oman-UAE Mountains. *Journal of Structural Geology*, *158*, 104594. https://doi.org/10.1016/j.jsg.2022.104594

Searle, M. P. (2007). Structural geometry, style and timing of deformation in the Hawasina window, Al Jabal Al Akhdar and Saih Hatat culminations, Oman Mountains. *GeoArabia*, *12*(2), 99–130. https://doi.org/10.1016/0040-1951(77)90059-2

Searle, M. P., & Cox, J. (2002). Subduction zone metamorphism during formation and emplacement of the Samail ophiolite in the Oman Mountains. *Geological Magazine*, *139*(3), 241–255. https://doi.org/10.1017/s0016756802006532

Searle, M. P., & Malpas, J. (1980). Structure and metamorphism of rocks beneath the Semail ophiolite of Oman and their significance in ophiolite obduction. *Transactions of the Royal Society of Edinburgh Earth Sciences*, *71*(4), 247–262. https://doi.org/10.1017/S0263593300013614

Searle, M. P., Warren, C. J., Waters, D. J., & Parrish, R. R. (2004). Structural evolution, metamorphism and restoration of the Arabian continental margin, Saih Hatat region, Oman Mountains. *Journal of Structural Geology*, *26*(3), 451–473. https://doi.org/10.1016/j.jsg.2003.08.005

Searle, M. P., Waters, D. J., Martin, H. N., & Rex, D. C. (1994). Structure and metamorphism of blueschist–eclogite facies rocks from the northeastern Oman Mountains. *Journal of the Geological Society of London*, *151*(3), 555–576. https://doi.org/10.1144/gsjgs.151.3.0555

Soret, M., Bonnet, G., Agard, P., Larson, K., Cottle, J., Dubacq, B., et al. (2022). Timescales of subduction initiation and evolution of subduction thermal regimes. *Earth and Planetary Science Letters*, *584*, 117521. https://doi.org/10.1016/j.epsl.2022.117521

Stern, R. J., & Bloomer, S. (1992). *Subduction zone infancy: Examples from the Eocene Izu-Bonin-Mariana and Jurassic California arcs* (Vol. 104, pp. 1621–1636). Geological Society of America Special Publications. https://doi.org/10.1017/CBO9781107415324.004

Stüwe, K., & Schuster, R. (2010). Initiation of subduction in the Alps: Continent or ocean? *Geology*, *38*(2), 175–178. https://doi.org/10.1130/G30528.1

Tilton, G. R., Hopson, C. A., & Wright, J. E. (1981). Uranium-lead isotopic ages of the Samail Ophiolite, Oman, with applications to Tethyan Ocean ridge tectonics. *Journal of Geophysical Research*, *86*(B4), 2763–2775. https://doi.org/10.1029/JB086iB04p02763

Turcotte, D. L., & Schubert, G. (2002). *Geodynamics* (2nd ed., p. 456). Cambridge University Press.

Van Hinsbergen, D. J., Peters, K., Maffione, M., Spakman, W., Guilmette, C., Thieulot, C., et al. (2015). Dynamics of intraoceanic subduction initiation: 2. Suprasubduction zone ophiolite formation and metamorphic sole exhumation in context of absolute plate motions. *Geochemistry, Geophysics, Geosystems*, *16*(6), 1771–1785. https://doi.org/10.1002/2015gc005745

van Hinsbergen, D. J. J., Maffione, M., Koornneef, L. M. T., & Guilmette, C. (2019). Kinematic and paleomagnetic restoration of the Semail ophiolite (Oman) reveals subduction initiation along an ancient Neotethyan fracture zone. *Earth and Planetary Science Letters*, *518*, 183–196. https://doi.org/10.1016/j.epsl.2019.04.038

van Hinsbergen, D. J. J., Steinberger, B., Guilmette, C., Maffione, M., Gurer, D., Peters, K., et al. (2021). A record of plume-induced plate rotation triggering subduction initiation. *Nature Geoscience*, *14*(8), 626–630. https://doi.org/10.1038/s41561-021-00780-7

Vitale Brovarone, A., & Herwartz, D. (2013). Timing of HP metamorphism in the Schistes Lustrès of Alpine Corsica: New Lu–Hf garnet and lawsonite ages. *Lithos*, *172*, 175–191. https://doi.org/10.1016/j.lithos.2013.03.009

Warren, C. J., Parrish, R. R., Searle, M. P., & Waters, D. J. (2003). Dating the subduction of the Arabian continental margin beneath the Semail Ophiolite, Oman. *Geology*, *31*(10), 89–892. https://doi.org/10.1130/g19666.1

Warren, C. J., Parrish, R. R., Waters, D. J., & Searle, M. P. (2005). Dating the geologic history of Oman's Semail Ophiolite: Insights from U-Pb geochronology. *Contributions to Mineralogy and Petrology*, *150*(4), 403–422. https://doi.org/10.1007/s00410-005-0028-5

Warren, C. J., Sherlock, S. C., & Kelley, S. P. (2011). Interpreting high pressure phengite $^{40}Ar/^{39}Ar$ laserprobe ages: An example from Saih Hatat, NE Oman. *Contributions to Mineralogy and Petrology*, *161*(6), 991–1009. https://doi.org/10.1007/s00410-010-0576-1

Weidle, C., Wiesenberg, L., El-Sharkawy, A., Krüger, F., Scharf, A., Agard, P., & Meier, T. (2022). A 3-D crustal shear wave velocity model and Moho map below the Semail Ophiolite, eastern Arabia. *Geophysical Journal International*, *231*(2), 817–834. https://doi.org/10.1093/gji/ggac223

References From the Supporting Information

Freeman, S. R., Butler, R. W. H., Cliff, R. A., & Rex, D. C. (1998). Direct dating of mylonite evolution: A multi-disciplinary geochronological study from the Moine Thrust Zone, NW Scotland. *Journal of the Geological Society*, *155*(5), 745-758. https://doi.org/10.1144/gsjgs.155.5.0745

Glodny, J., Ring, U., & Kühn, A. (2008). Coeval high-pressure metamorphism, thrusting, strike-slip, and extensional shearing in the Tauern Window, Eastern Alps. *Tectonics*, *27*(4). https://doi.org/10.1029/2007TC002193

Inger, S., & Cliff, R. A. (1994). Timing of metamorphism in the Tauern Window, Eastern Alps: Rb-Sr ages and fabric formation. *Journal of metamorphic Geology*, *12*(5), 695-707.

Ludwig, K. R. (2009). *Isoplot/Ex Ver 3.71: A geochronological toolkit for Microsoft Excel*. Berkeley Geochronology Center Special Publication, Berkeley.

Villa, I. M., De Bièvre, P., Holden, N. E., & Renne, P. R. (2015). IUPAC-IUGS recommendation on the half life of ^{87}Rb. *Geochimica et Cosmochimica Acta*, *164*, 382-385. https://doi.org/10.1016/j.gca.2015.05.025